

Sparse Sensing, Communication, and Actuation via Self-Triggered Control Algorithms

MirSaleh Bahavarnia ^{a,*}, Hossein K. Mousavi ^b, Nader Motee ^b

^aDepartment of Electrical and Computer Engineering and Institute for Systems Research, University of Maryland at College Park, USA

^bDepartment of Mechanical Engineering and Mechanics, Lehigh University, Bethlehem, USA

Abstract

We propose a self-triggered control algorithm to reduce onboard processor usage, communication bandwidth, and energy consumption across a linear time-invariant networked control system. We formulate an optimal control problem by penalizing the ℓ_0 -measures of the feedback gain and the vector of control inputs and maximizing the dwell time between the consecutive triggering times. It is shown that the corresponding ℓ_1 -relaxation of the optimal control problem is feasible and results in a stabilizing feedback control law with guaranteed performance bounds, while providing a sparse schedule for collecting samples from sensors, communication with other subsystems, and activating the input actuators.

1 Introduction

The design of feedback control strategies with sparse communication topologies has been one of the active research areas in networked control systems in recent years [1,3,8,11], where the control objective is to find a sparse state feedback gain by minimizing a ℓ_1 -regularized, which is usually quadratic, cost functional. Promoting sparsity in the state feedback gain results in a reduced communication requirement among the subsystems, which is practically plausible in networked systems with limited onboard resources (e.g., short battery life on quadcopters). In this paper, we take further steps and enhance sparsity by using a self-triggered state feedback control mechanism and allowing subsystems to sense less frequently, communicate whenever performance deteriorates below some pre-specified threshold, and activate their actuators if necessary.

The fundamental idea of the self-triggered control is to reduce the need for continuous sensing and actuation by incurring some performance loss in a controlled manner. A performance-preserving condition or Lyapunov-based stability condition, which is known as the self-triggering condition, is usually verified to determine whether new updates are necessary or not. In this approach, the next update time is solely computed based on the current state information [6,4].

In [14], the problem of linear time-invariant networked systems with limited bandwidth on their communication channels is considered, where the authors develop a self-triggered method to schedule sampling instances as well as switching times of feedback gains with \mathcal{H}_2 and \mathcal{H}_∞ performance guarantees. In [13], the authors employ ideas from the self-triggered control to develop an algorithm for a network of multiple agents on how to collect new samples and compute localized control inputs in order to achieve optimal static deployment in a given convex region. The authors of [12] show that if the sparsest control signal for a finite-horizon optimal control is unique, then the corresponding ℓ_1 -regularized optimal control problem recovers the sparsest solution. They leverage this idea and design a sparse self-triggered control law for linear time-invariant systems. In [7], the L^p control problems with $0 < p < 1$ is considered, where the authors obtain a maximum principle and conditions for the existence of solution for optimal control problems with L^0 -regularized quadratic costs. In [4], the triggering times and feedback gains for the quadratic optimal control of linear time-invariant systems are designed with guaranteed performance bounds.

In this paper, we propose a control algorithm that is based on ideas from sparse feedback control and self-triggered control design techniques to achieve higher levels of sparsity, both in time and space, by reducing sensing, communication, and input actuation requirements with a prescribed performance bound. To achieve these goals, in Sections 2 and 3, we formulate an optimal control problem in which subsystems measure their own state variables and then share them over a (time-varying) communication topology. Each subsystem receives the state information of other neighboring

* The corresponding author is M. Bahavarnia.

Email addresses: mbahavar@umd.edu (MirSaleh Bahavarnia), mousavi@lehigh.edu (Hossein K. Mousavi), motee@lehigh.edu (Nader Motee).

subsystems once (at triggering times) and forms its optimal control input using these samples and apply it for some period of time without updating it. As soon as the performance deteriorates below some threshold, subsystems trigger and collect new samples and repeat the process. The control inputs are formed using state feedback gains that are computed by minimizing a cost function that is penalized by the ℓ_0 -measures of the feedback gain and the vector of control inputs. In Section 4, we show that this optimal control problem and its ℓ_1 -relaxation are feasible. To prolong the triggering intervals, where over which new samples will not be collected and feedback gains stay fixed, our algorithm in Section 5 solves a nonlinear optimization problem for the next triggering time. Then, using this value, a ℓ_1 -relaxation of the optimal control problem is solved to find a sparse feedback gain. In the last step, the value of the next triggering time is corrected using this feedback gain. It is shown that the resulting feedback control strategy is stabilizing and provides guaranteed performance bounds. The usefulness of our theoretical findings is verified through extensive simulations in Section 6. This paper is an outgrowth of [2] with several updated and new results and simulations.

Notations: The set of real numbers, positive real numbers, positive integer numbers, and non-negative integer numbers are denoted by \mathbb{R} , \mathbb{R}_{++} , \mathbb{N} , and \mathbb{Z}_+ , respectively. The supremum of a subset of \mathbb{R} is denoted by \sup . For a function of time $f(t)$, $f'(t) = \partial f(t)/\partial t$. The positive semi-definiteness and positive-definiteness are denoted by $\succeq 0$ and $\succ 0$, respectively. The identity matrix is represented by I . The Euclidean norm of vector v is denoted by $\|v\|_2$. The cardinality (ℓ_0 sparsity measure), ℓ_1 norm, and largest singular value of a matrix M are represented by $\|M\|_0$, $\|M\|_1$, and $\|M\|$, respectively, where $\|M\|_0$ is identical to its number of nonzero elements and $\|M\|_1$ is the sum of absolute values of its elements. A matrix is called Hurwitz if all of its eigenvalues have negative real parts. The vectorization and determinant of a matrix M are denoted by $\text{vec}(M)$ and $\det(M)$, respectively. The Kronecker product is denoted by \otimes .

2 Problem Statement

We consider the linear time-invariant (LTI) control systems described by

$$\dot{x}(t) = Ax(t) + Bu(t), \quad x(0) = x_0, \quad (1)$$

where $x \in \mathbb{R}^n$ denotes the state vector, $u \in \mathbb{R}^m$ represents the control input, and x_0 is the initial state. To stabilize system (1) and regularize $x(t)$ toward the origin, we use the sample-and-hold feedback control laws

$$u(t) = u_k := F_k x(t_k) = F_k x_k, \quad (2)$$

for all $t \in [t_k, t_{k+1})$, in which the sequence of time instants $\{t_k\}_{k=0}^\infty \subset \mathbb{R}_+$ are called triggering times, and $[t_k, t_{k+1})$ is the k 'th time interval. The resulting sequence of inter-

execution times is $\{\delta_k\}_{k=0}^\infty$, wherein

$$\delta_k := t_{k+1} - t_k. \quad (3)$$

The sequence of feedback gains is also denoted by $\{F_k\}_{k=1}^\infty \subset \mathbb{R}^{m \times n}$. The cost-to-go $J_k(F_k, \xi; x_k)$ corresponding to time interval $[t_k, t_k + \xi)$ is

$$J_k(F_k, \xi; x_k) := \int_{t_k}^{t_k + \xi} \left(x(t)^T Q x(t) + u(t)^T R u(t) \right) dt \quad (4)$$

for all $\xi \in [0, \delta_k)$ and weight matrices $Q \succ 0$ and $R \succ 0$.

Assumption 1 *The pair (A, B) is stabilizable.*

Since $Q \succ 0$ and Assumption 1 holds, the LQR problem corresponding to cost functional (4) has a unique stabilizing solution. For a pre-designed and stabilizing feedback gain \tilde{F} , the infinite-horizon cost value is given by

$$\tilde{J}(x_0) := x_0^T \tilde{P} x_0, \quad (5)$$

where $\tilde{P} \succ 0$ is the unique solution to Lyapunov equation

$$\left(A + B\tilde{F} \right)^T \tilde{P} + \tilde{P} \left(A + B\tilde{F} \right) + Q + \tilde{F}^T R \tilde{F} = 0. \quad (6)$$

This solution exists because $A + B\tilde{F}$ is Hurwitz and $Q + \tilde{F}^T R \tilde{F} \succ 0$. A popular choice for \tilde{F} is the standard linear quadratic regulator (LQR). In the traditional controller design methods, \tilde{F} is usually non-sparse; i.e., most of its elements are nonzero.

The *problem* is to design the sequences of inter-execution times $\{\delta_k\}_{k=0}^\infty$ and feedback gains $\{F_k\}_{k=0}^\infty$ in order to ensure the following control objectives: (i) sparse sensing both in space and time, (ii) sparse scheduling of actuators, and (iii) guaranteed stability and closed-loop performance compared to a well-performing feedback gain \tilde{F} .

3 Initial Problem Developments

We show how the objectives of the paper can be translated to an optimization problem. To achieve objective (i), one can maximize the inter-execution time δ_k and minimize $\|F_k\|_0$. To realize objective (ii), we may minimize $\|u_k\|_0$, which is the number of actuators that is used in interval $[t_k, t_{k+1})$. To achieve objective (iii), we consider a Lyapunov-based performance and stability analysis, which is a well-investigated methodology in model predictive control (MPC) (e.g., see [4]). First, the total cost value is given by

$$J(x_0) := \sum_{k=0}^{\infty} J_k(F_k, \delta_k; x_k). \quad (7)$$

The relative performance loss with respect to the benchmark cost value (5) is

$$\nu(x_0) := \frac{J(x_0) - \tilde{J}(x_0)}{\tilde{J}(x_0)}. \quad (8)$$

Theorem 1 Suppose that for some given $\alpha > 1$, the sequences of triggering times, $\{t_k\}_{k=0}^{\infty}$, inter-execution times $\{\delta_k\}_{k=0}^{\infty}$, and feedback gains $\{F_k\}_{k=0}^{\infty}$, inequality

$$J_k(F_k, \xi; x_k) \leq \alpha (V(x(t_k)) - V(x(t_k + \xi))), \quad (9)$$

holds for every $\xi \in [0, \delta_k]$, in which the Lyapunov function $V : \mathbb{R}^n \rightarrow \mathbb{R}$ is defined as

$$V(x(t)) := x(t)^T \tilde{P} x(t).$$

Then, control law (2) is stabilizing. Moreover, for all $x_0 \in \mathbb{R}^n$, the relative performance loss $\nu(x_0)$ satisfies

$$\nu(x_0) \leq \alpha - 1. \quad (10)$$

Proof: Let us define $S_N := \sum_{k=0}^N J_k(F_k, \delta_k; x_k)$. We can use (9) and the limit of $\xi \rightarrow \delta_k$ for each term to get

$$\begin{aligned} S_N &\leq \sum_{k=0}^N \alpha (V(x_k) - V(x_{k+1})) \\ &= \alpha (V(x_0) - V(x_N)) < \alpha V(x_0) = \alpha \tilde{J}(x_0). \end{aligned}$$

Since $\{S_N\}_{N=0}^{\infty}$ is a nondecreasing sequence that is bounded from above, it has a limit, that is actually $J(x_0)$. Moreover,

$$J(x_0) = \lim_{N \rightarrow \infty} S_N \leq \alpha \tilde{J}(x_0). \quad (11)$$

A simple reorganization of (11) reveals that (10) holds. \square

We combine these objectives and formulate the self-triggered sparse optimal control problem as

$$\begin{aligned} &\underset{F_k, \delta_k}{\text{minimize}} && -\delta_k + \gamma \|F_k\|_0 + \eta \|u_k\|_0 && \text{(P1)} \\ &\text{subject to :} && (1) \text{ and } (2), \\ &&& (9) \text{ for all } \xi \in [0, \delta_k] \end{aligned}$$

The nonnegative parameters γ and η adjust the balance between the levels of spatial and temporal sparsity in terms of sensing and actuation, respectively.

Theorem 2 Every feasible solution of problem (P1) is a stabilizing control law with performance guarantee (10).

Remark 1 The method proposed by [6] solely takes advantage of the Lyapunov function evolutions. However, our

proposed problem setup resembles the method proposed by [4], in which in addition to the Lyapunov functions, a performance-based condition is utilized.

4 Equivalent Formulation, Relaxation, and Feasibility

We show that (P1) can be reformulated as a regularized quadratically-constrained quadratic program (QCQP) when δ_k is kept fixed. Then, we suggest appropriate relaxations that make the problem more tractable.

Lemma 1 For all $k \in \mathbb{N}$ and $j \in \mathbb{Z}_+$, feedback control law (2) can be decomposed as

$$u(t) = F_k N_k x_0$$

for all $t \in [t_k, t_{k+1})$, where $N_0 := I$ and N_k is recursively given by

$$N_k := M_{k-1}(\delta_{k-1}) N_{k-1}$$

and the matrices M_j 's are given by

$$M_j(\xi) := e^{A\xi} (I + Z(\xi) B F_j), \quad Z(\xi) := \int_0^\xi e^{-A\tau} d\tau.$$

Proof: Solving system (1) together with (2) for time interval $[t_k, t_{k+1})$ gives us

$$\begin{aligned} x(t) &= e^{A(t-t_k)} x(t_k) + \int_{t_k}^t e^{A(t-\phi)} B F_k x(t_k) d\phi \\ &= e^{A(t-t_k)} \left(I + \int_0^{t-t_k} e^{A(-\tau)} B F_k d\tau \right) x(t_k) \\ &= e^{A(t-t_k)} (I + Z(t-t_k) B F_k) x(t_k) \\ &= M_k(t-t_k) x(t_k). \end{aligned}$$

Since $x(t)$ is continuous at $t = t_{k+1}$, thus

$$x(t_{k+1}) = e^{A\delta_k} (I + Z(\delta_k) B F_k) x(t_k) = M_k(\delta_k) x(t_k).$$

By induction, $x(t_k) = N_k x_0$. \square

We derive a quadratic form for the cost-to-go.

Lemma 2 The k 'th time interval cost $J_k(F_k, \xi; x_k)$ can be expressed as the quadratic term

$$J_k(F_k, \xi; x_k) = x_k^T Y_k(F_k, \xi) x_k,$$

where the matrix Y_k is given by

$$Y_k(F_k, \xi) := H_0(\xi) + F_k^T H_1(\xi)^T + H_1(\xi) F_k + F_k^T H_2(\xi) F_k,$$

for all $k \in \mathbb{Z}_+$ and

$$\begin{aligned} H_0(\xi) &:= \int_0^\xi e^{A^T \tau} Q e^{A \tau} d\tau, \\ H_1(\xi) &:= \int_0^\xi e^{A^T \tau} Q e^{A \tau} Z(\tau) B d\tau, \\ H_2(\xi) &:= \int_0^\xi (e^{A^T \tau} Z(\tau) B)^T Q (e^{A \tau} Z(\tau) B) d\tau + \xi R. \end{aligned}$$

Proof. We can write

$$J_k(F_k, \xi; x_k) = J_k^x(F_k, \xi; x_k) + J_k^u(F_k, \xi; x_k),$$

wherein

$$\begin{aligned} J_k^x(F_k, \xi; x_k) &= \int_{t_k}^{t_k+\xi} x_k^T M_k(t-t_k)^T Q M_k(t-t_k) x_k dt \\ &= x_k^T \int_0^\xi M_k(\tau)^T Q M_k(\tau) d\tau x_k \end{aligned}$$

and

$$J_k^u(F_k, \xi; x_k) = \int_{t_k}^{t_k+\xi} x_k^T F_k^T R F_k x_k dt = x_k^T (\xi F_k^T R F_k) x_k.$$

Then, we get $J_k(F_k, \xi; x_k) = x_k^T Y_k(F_k, \xi) x_k$, wherein

$$Y_k(F_k, \xi) = \int_0^\xi M_k(\tau)^T Q M_k(\tau) d\tau + \xi_k F_k^T R F_k. \quad (12)$$

The claim follows by substituting $M_k(\tau) = e^{A^T (I + Z(\tau) B F_k)}$ in the right side of (12). \square

When δ_k is kept fixed, the following proposition states an important property about matrix $H_2(\xi)$ which leads to the convex reformulation of **(P1)** (in terms of variable F_k).

Proposition 1 For all $\xi > 0$, $H_2(\xi)$ is positive-definite.

Proof. For arbitrary nonzero vector $v \in \mathbb{R}^m$, we get

$$\begin{aligned} &v^T H_2(\xi) v \\ &= v^T \left(\int_0^\xi (e^{A^T Z(\tau) B})^T Q (e^{A^T Z(\tau) B}) d\tau + \xi R \right) v \\ &= \int_0^\xi (e^{A^T Z(\tau) B} v)^T Q (e^{A^T Z(\tau) B} v) d\tau + \xi v^T R v. \end{aligned}$$

Since $Q \succ 0$, the last integrand is non-negative. Therefore, the integral is also non-negative. Since $R \succ 0$, $\xi v^T R v > 0$. Thus, $v^T H_2(\xi) v > 0$ and the conclusion follows. \square

Now, we can state the following equivalent formulation.

Theorem 3 The optimization problem **(P1)** is equivalent to

$$\begin{aligned} &\underset{f_k, \delta_k}{\text{minimize}} \quad -\delta_k + \gamma \|f_k\|_0 + \eta \|(x_k^T \otimes I) f_k\|_0 \quad (\mathbf{P2}) \\ &\text{subject to : for all } \xi \in [0, \delta_k] : \quad (13) \\ &\quad \frac{1}{2} f_k^T P_1(\xi) f_k + q_1(\xi)^T f_k + r_1(\xi) \leq 0, \end{aligned}$$

where $f_k := \text{vec}(F_k)$ and

$$\begin{aligned} P_1(\xi) &:= 2(x_k x_k^T) \otimes (H_2(\xi) + \alpha B^T Z(\xi)^T e^{A^T \xi} \tilde{P} e^{A \xi} Z(\xi) B), \\ q_1(\xi) &:= 2 \text{vec} \left((H_1(\xi)^T + \alpha B^T Z(\xi)^T e^{A^T \xi} \tilde{P} e^{A \xi}) x_k x_k^T \right), \\ r_1(\xi) &:= x_k^T (H_0(\xi) + \alpha (e^{A^T \xi} \tilde{P} e^{A \xi} - \tilde{P})) x_k. \end{aligned}$$

Proof. The building block of the proof is the identity

$$\text{vec}(UVW) = (W^T \otimes U) \text{vec}(V) \quad (14)$$

for any triplet (U, V, W) . Using (14) for $U = I$, $V = F_k$, and $W = x_k$, the objective function of **(P1)** takes the form of objective function in **(P2)**. Likewise, by repeated application of (14) on (9), one can verify (15). \square

If we combine Theorem 3 and of Proposition 1, we observe that constraint (15) involves a quadratic convex function of variable $f_k = \text{vec}(F_k)$. Thus, when δ_k is kept fixed, **(P2)** takes the form of a regularized QCQP. Next, we relax **(P2)** by replacing the ℓ_0 -norm with its convex surrogate the ℓ_1 -norm to get the following form.

$$\begin{aligned} &\underset{f_k, \delta_k}{\text{minimize}} \quad -\delta_k + \gamma \|f_k\|_1 + \eta \|(x_k^T \otimes I) f_k\|_1 \quad (\mathbf{P3}) \\ &\text{subject to : for all } \xi \in [0, \delta_k] : \quad (15) \\ &\quad \frac{1}{2} f_k^T P_1(\xi) f_k + q_1(\xi)^T f_k + r_1(\xi) \leq 0, \end{aligned}$$

Although the ℓ_1 -relaxation makes **(P2)** more tractable, the left hand side of constraint **(P3)** may be still a nonconvex function of ξ . Thus, solving **(P3)** for optimal solutions generally remains a difficult non-convex task. In order to sub-optimally solve **(P3)** we propose a two-stage method that is discussed in Section 5. The constraints of relaxed problem **(P3)** and the original problem **(P1)** are identical. Moreover, stability and performance guarantees of **(P1)** originate from its constraint. Hence, their feasibility, stability, and performance guarantee are equivalent.

Theorem 4 The feasible solutions to **(P3)** are feasible solutions to **(P1)**. Moreover, any solution to **(P3)** results in a stabilizing control (2) law with performance guarantee (10).

We prove the feasibility of these optimization problems.

Theorem 5 For every $\alpha > 1$, problem **(P1)** and its relaxation **(P3)** are feasible.

Proof: (9) is equivalent to $g(\xi; F_k) \leq 0$, where

$$g(\xi; F_k) := x_k^T \left(Y_k(F_k, \xi) + \alpha(-\tilde{P} + M_k(\xi)^T \tilde{P} M_k(\xi)) \right) x_k.$$

We can show that $g'(0; F_k) = x_k^T W_k x_k$, in which

$$W_k = Q + F_k^T R F_k + \alpha((A + B F_k)^T \tilde{P} + \tilde{P}(A + B F_k)).$$

According to (6), we get

$$g'(0; \tilde{F}) = (1 - \alpha) x_k^T \left(Q + \tilde{F}^T R \tilde{F} \right) x_k.$$

Since $\alpha > 1$ and $Q + \tilde{F}^T R \tilde{F} \succ 0$, we get $g'(0; \tilde{F}) < 0$. In addition, $g(0; \tilde{F}) = 0$. Therefore, there exists a positive θ_k at $F_k = \tilde{F}$ such that for all $\xi \in (0, \theta_k)$ we have $g(\xi; \tilde{F}) < 0$. This proves the feasibility of **(P1)**. Using Theorem 4 the feasibility of **(P3)** is followed as well. \square

5 Self-Triggered Sparse Optimal Control

We find a sequence of stabilizing feedback gains and inter-execution times that satisfy desired performance guarantees.

5.1 Solving **(P3)** for δ_k while F_k is Fixed

This concerns a subproblem that is a component of our algorithm. Inequality (15) is equivalent to the constraint

$$\frac{1}{2} u_k^T P_2(\xi) u_k + q_2(\xi)^T u_k + r_1(\xi) \leq 0, \quad (16)$$

where $u_k := F_k x_k$ and

$$\begin{aligned} P_2(\xi) &:= 2H_2(\xi) + 2\alpha B^T Z(\xi)^T e^{A^T \xi} \tilde{P} e^{A \xi} Z(\xi) B, \\ q_2(\xi) &:= \left(2H_1(\xi)^T + 2\alpha B^T Z(\xi)^T e^{A^T \xi} \tilde{P} e^{A \xi} \right) x_k. \end{aligned}$$

When we fix feedback gain F_k , **(P3)** becomes equivalent to the nonlinear optimization problem

$$\begin{aligned} &\underset{\delta_k}{\text{maximize}} \quad \delta_k && \text{(P4)} \\ &\text{subject to :} && \text{(16) for every } \xi \in [0, \delta_k]. \end{aligned}$$

The optimal solution of **(P4)** can be characterized by

$$\delta_k^* = \sup \left\{ \theta_k > 0 \mid (16) \text{ holds for all } \xi \in [0, \theta_k] \right\}. \quad (17)$$

In order to solve (17), we utilize the simple and commonly-used discretization rule with fixed step-size, e.g., see [9,6]. The general nonlinear optimization methods can be effective to solve (17) as well. In the rest of this paper, we suppose that there exists a procedure $\text{InterExec}(F_k)$ that solves **(P4)** for a fixed gain F_k and returns δ_k^* .

5.2 Solving for F_k when δ_k is Fixed

When δ_k is kept fixed, solving **(P3)** for F_k is still an infinite-dimensional optimization. Therefore, we relax the problem by evaluating (16) only at $\xi = \delta_k$ and ensuring the feasibility of **(P4)** after updating F_k by imposing an additional constraint. Applying the Schur complement to (16) and setting the argument ξ to δ_k , we arrive at the LMI constraint

$$\begin{bmatrix} 2P_2(\delta_k)^{-1} & F_k x_k \\ x_k^T F_k^T & -q_2(\delta_k)^T F_k x_k - r_1(\delta_k) \end{bmatrix} \succeq 0. \quad (18)$$

Proposition 2 Suppose that F_k satisfies

$$\begin{bmatrix} R^{-1} & F_k \\ F_k^T & -\alpha((A + B F_k)^T \tilde{P} + \tilde{P}(A + B F_k)) - Q \end{bmatrix} \succ 0. \quad (19)$$

Then, **(P4)** for feedback gain F_k is feasible.

Proof: If $g'(0; F_k) < 0$, then using the same argument given in the proof of Theorem 5, **(P4)** would be feasible. One inspects that inequality $g'(0; F_k) < 0$ is equivalent to

$$x_k^T (Q + F_k^T R F_k + \alpha((A + B F_k)^T \tilde{P} + \tilde{P}(A + B F_k))) x_k < 0.$$

For this inequality to hold independent of x_k , we need

$$Q + F_k^T R F_k + \alpha((A + B F_k)^T \tilde{P} + \tilde{P}(A + B F_k)) \prec 0. \quad (20)$$

Applying the Schur complement to (20), we obtain (19). \square

Solving the two LMIs (18) and LMI (19) together with our objective function, we arrive at a semi-definite program

$$\begin{aligned} F_k^* &= \underset{F_k}{\text{argmin.}} \quad \gamma \|F_k\|_1 + \eta \|F_k x_k\|_1 && \text{(P5)} \\ &\text{subject to :} && \text{LMI (18) and LMI (19),} \end{aligned}$$

The gain F_k that is obtained from **(P5)** may not satisfy inequality (15) for all $\xi \in [0, \delta_k]$ that may arise from ignoring the continuous satisfaction of the constraint. To remedy this, we leverage (17) and modify the value of δ_k for the updated value of F_k (see the next subsection). In the rest of this paper, we suppose that there exists a procedure $\text{FeedbackGain}(\delta_k)$ that solves **(P5)** for a fixed δ_k and returns F_k^* .

5.3 Algorithm

Based on the discussions of the previous subsection, our control design algorithm consists of the following three steps: (i) solve **(P4)** to find the first estimate of δ_k for fixed $F_k = \tilde{F}$, (ii) for a fixed value of δ_k , find a value for F_k using **(P5)**, and (iii) for the updated value of feedback gain F_k , correct the value of $\delta_k = \delta_k^*$ using **(P4)**. These steps are summarized in Algorithm 1.

Algorithm 1 Self-Triggered Sparse Optimal Control

input: A, B, Q, R, γ, η , and α .

output: $\{F_k\}_{k=0}^\infty, \{\delta_k\}_{k=0}^\infty$, and $\{t_k\}_{k=0}^\infty$
initialize: $t_0 = 0, N_0 \leftarrow I$, evaluate $e^{A\xi}, H_0(\xi), H_1(\xi), H_2(\xi)$, and $Z(\xi)$ offline and save them in a look-up table

for $k = 0$ to ∞ **do**
 $F_k \leftarrow \tilde{F}$
 $\delta_k \leftarrow \text{InterExec}(F_k)$
 $F_k \leftarrow \text{FeedbackGain}(\delta_k)$
 $\delta_k \leftarrow \text{InterExec}(F_k)$
 $M_k(\delta_k) \leftarrow e^{A\delta_k}(I + Z(\delta_k)BF_k)$
 $N_{k+1} \leftarrow M_k(\delta_k)N_k, t_{k+1} \leftarrow t_k + \delta_k$
end for

Theorem 6 The sequences of feedback gains $\{F_k\}_{k=0}^\infty$ and triggering times $\{t_k\}_{k=0}^\infty$ resulting from Algorithm 1 gives a stabilizing control law

$$u(t) = F_k x_k, \quad (21)$$

for all $t \in [t_k, t_{k+1})$. Moreover, for all $x_0 \in \mathbb{R}^n$, the relative performance loss $\nu(x_0)$ satisfies

$$\nu(x_0) \leq \alpha - 1. \quad (22)$$

Proof: Because LMI (19) has been incorporated, for the derived value of $F_k, g'(0; F_k) < 0$, thus, the corresponding value of δ_k^* is strictly positive. Since for F_k and $\delta_k = \delta_k^*$, the constraint of the problem (16) is satisfied, (22) holds. \square

Optimal control problem (P5) can be solved by a convex optimization toolbox such as CVX [5].

Remark 2 Matrices $e^{A\xi}, Z(\xi), H_0(\xi), H_1(\xi)$ and $H_2(\xi)$ can be computed offline and over a grid with arbitrary resolution, as their values only depend on the state-space matrices, A and B , weight matrices, Q and R , and time argument, ξ . Then, during the execution, we can use look-up tables to enhance the computational complexity of our algorithm.

6 Numerical Simulations

To assess the effectiveness of the proposed procedure, we consider a class of spatially distributed systems (see [10] for more details). We consider a system of $N = 10$ subsystems, which are randomly placed in the region $[0, 10] \times [0, 10]$; see Fig. 1, in which each shape represents a subsystem. Then, the dynamics of i 'th subsystem is characterized by

$$\dot{x}^{(i)}(t) = [A]_{ii}x^{(i)}(t) + \sum_{\substack{j=1, \\ j \neq i}}^N [A]_{ij}x^{(j)}(t) + [B]_{ii}u^{(i)}(t),$$

where

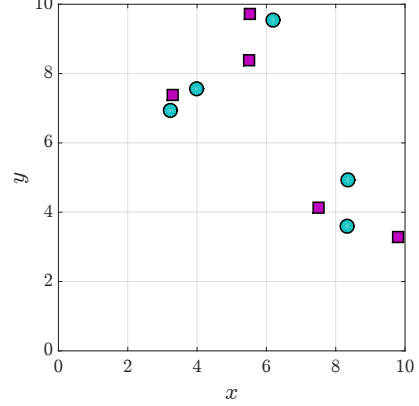


Fig. 1. Randomly generated positions of $N = 10$ subsystems.

$$[A]_{ii} = \begin{bmatrix} 1 & 1 \\ 1 & 2 \end{bmatrix}, [B]_{ii} = \begin{bmatrix} 0 \\ 1 \end{bmatrix} \text{ for square shapes,}$$

$$[A]_{ii} = \begin{bmatrix} -2 & 1 \\ 1 & -3 \end{bmatrix}, [B]_{ii} = \begin{bmatrix} 0 \\ 1 \end{bmatrix} \text{ for circle shapes,}$$

$$[A]_{ij} = \frac{1}{e^{\beta \text{dis}(i,j)}} \begin{bmatrix} 1 & 0 \\ 0 & 1 \end{bmatrix}, [B]_{ij} = \begin{bmatrix} 0 \\ 0 \end{bmatrix}, \forall j \neq i,$$

where β determines the rate of decay in the couplings and $\text{dis}(i, j)$ denotes the Euclidean distance between nodes i and j in \mathbb{R}^2 . The resulting system is of dimension $n = 20$. We set $\beta = 1, \gamma = \eta = 0.001, \alpha = 1.15, Q = I$, and $R = 2I$. We apply Algorithm 1 with $k_{\max} = 49$ iterations in the **for** loop and obtain Figures 2a and 2b, which depict the relative cardinality of feedback gains given by

$$\kappa_k := 100 \|F_k\|_0 / \|\tilde{F}\|_0, \quad (23)$$

and relative cardinality of control input vectors:

$$\mu_k := 100 \|u_k\|_0 / \|\tilde{u}_k\|_0, \quad (24)$$

respectively. Figures 2a and 2b illustrate that this method improves the spatial sparsity compared to the periodic feedback control with $F_k = \tilde{F}$ for all time intervals. In average, the cardinalities of F_k and u_k have almost decreased by 38% and 50%, respectively, while we lose about 15% in performance. Fig. 3a compares $\|x\|_2$ for two designs: our method and periodic time-triggered LQR design. In Fig. 3b, we illustrate the state of the system using the time-triggered design, starting from an initial state. Fig. 4 shows the inter-execution times δ_k versus time t . To measure the average relative cardinality of feedback gains over time, we define

$$R_F := \frac{\sum_{k=0}^{k_{\max}} \delta_k \kappa_k}{\sum_{k=0}^{k_{\max}} \delta_k},$$

which represents the average sensor activity throughout time. Likewise, the average relative cardinality of control

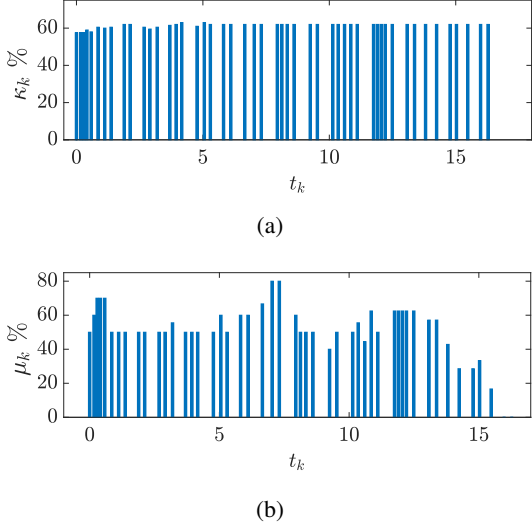


Fig. 2. (a) Relative cardinality of controllers κ_k defined in (23) versus triggering times t_k (b) Relative cardinality of control inputs μ_k defined in (24) versus triggering times t_k .

inputs over time is defined as

$$R_u := \frac{\sum_{k=0}^{k_{\max}} \delta_k \mu_k}{\sum_{k=0}^{k_{\max}} \delta_k},$$

which represents the average actuator activity throughout time. Also, the average inter-execution time is $D := (\sum_{k=0}^{k_{\max}} \delta_k) / k_{\max}$, that quantifies the time sparsity of (state) sampling. The dependency of these quantities on α is captured in Table 1, which demonstrates that by accepting higher levels of performance loss, we achieve sparser control designs in terms of both sensing and actuation activity (i.e., smaller values of R_F and R_u) and sampling activity in time (i.e., larger values of D). In the next simulations, we preserve the parameters except for β . Figures 5a, 5b, and 6 demonstrate the dependency of R_F , R_u , and D on β , respectively. Fig. 5a and Fig. 5b depict that there is a tradeoff between the spatial decay rate β and the indices of sensing and actuating activity, R_F and R_u : as β increases, the system tends to be more localized and, consequently, F_k 's and u_k 's become sparser. Moreover, according to Fig. 6, as the system gets more localized, the average inter-execution time increases; i.e., less number of samples are required on average (in time).

We consider the previous setup and study the effect of penalizing parameters γ and η . To investigate the effect of γ on R_F , we set $\alpha = 1.15$ (i.e., accepting at most 15% performance loss), $\eta = 0.001$, and vary γ in $[10^{-5}, 10^{-3}]$. The result of Algorithm 1 shows that R_F decreases as γ grows (see Fig. 7a), which implies that the average sensing requirements of the subsystems from each other has decreased. We repeat the previous study for fixed value of $\gamma = 10^{-3}$ and by varying η in $[10^{-5}, 10^{-3}]$. Fig. 7b illustrates the relationship between η and R_u . Similar to (R_F, γ) relationship,

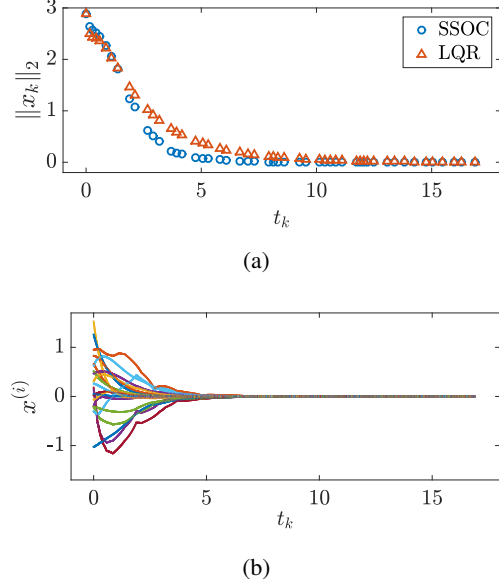


Fig. 3. (a) The Euclidean norm of state trajectories of SSOC and periodic time-triggered LQR design $\|x_k\|_2$ versus triggering times t_k (b) state trajectories $x^{(i)}$'s of our design with a random x_0

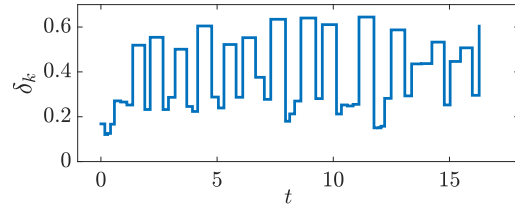


Fig. 4. Inter-execution times δ_k versus time t .

Table 1

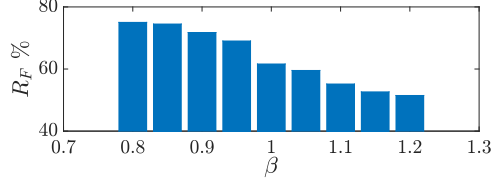
Dependency of quantities R_F , R_u , and D on parameter α .

α	R_F	R_u	D
1.05	85.56%	62.54%	0.2823
1.10	72.60%	66.89%	0.2715
1.15	61.61%	49.67%	0.3322
1.20	53.86%	41.04%	0.3247
1.25	50.63%	36.81%	0.3629
1.30	49.05%	32.00%	0.3529

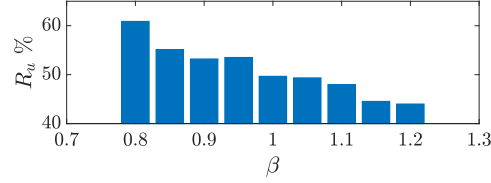
there exists a tradeoff between R_u and η : as η increases, on average, it enforces more components of u_k to be zero; i.e., less number of actuators on average are utilized (in time).

7 Discussion and Conclusion

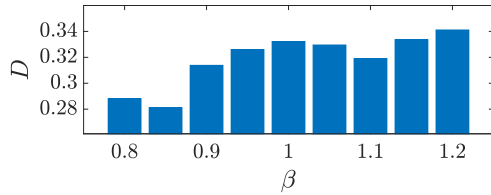
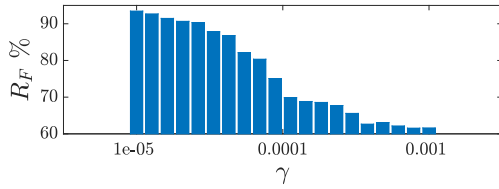
We present a control algorithm based on blending ideas from self-triggered control and ℓ_1 -regularized optimal control. The cornerstones of our algorithm are: estimation of



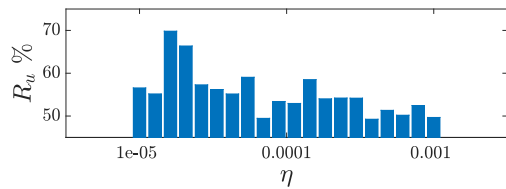
(a)



(b)

Fig. 5. (a) R_F versus decay rate β . (b) R_u versus decay rate β .Fig. 6. Average inter-execution time D versus spatial decay rate β .

(a)



(b)

Fig. 7. (a) R_F versus penalizing parameter γ . (b) R_u versus penalizing parameter η .

the inter-execution time while feedback gain is kept fixed (via a nonlinear optimization), design of the sparse optimal controller while inter-execution time is kept fixed (via a convex optimization), and correcting the value of the next triggering times using the resulting feedback gain. The closed-loop stability is guaranteed by imposing a performance-ensuring constraint. Our extensive numerical simulations assert that our proposed algorithm improves space-time sparsity in sensing, communication, and actuation in an interconnected network of multiple systems. In the case of spa-

tially decaying systems, our simulations show that there exists a tradeoff between the spatial decay rate and sparsity of the communication graph (i.e., sparsity of the feedback gains). Likewise, as the spatial decay rate increases, the average sampling rate decreases. One of our future research directions is to modify our algorithm and implement it in a distributed and asynchronous manner using localized information.

Acknowledgment

The authors would like to thank Prof. Paulo Tabuada for his fruitful comments and discussions.

References

- [1] Reza Arastoo, MirSaleh Bahavarnia, Mayuresh V Kothare, and Nader Motee. Closed-loop feedback sparsification under parametric uncertainties. In *IEEE 55th Conference on Decision and Control (CDC)*, pages 123–128, 2016.
- [2] MirSaleh Bahavarnia, Paulo Tabuada, Christoforos Somarakis, and Nader Motee. Improving sparsity in time and space via self-triggered sparse optimal controllers. In *IEEE 56th Annual Conference on Decision and Control (CDC)*, pages 4199–4204, 2017.
- [3] Ghazal Fazelnia, Ramtin Madani, Abdulrahman Kalbat, and Javad Lavaei. Convex relaxation for optimal distributed control problems. *IEEE Transactions on Automatic Control*, 62(1):206–221, 2017.
- [4] Tom Gommans, Duarte Antunes, Tijs Donkers, Paulo Tabuada, and Maurice Heemels. Self-triggered linear quadratic control. *Automatica*, 50(4):1279–1287, 2014.
- [5] Michael Grant, Stephen Boyd, and Yinyu Ye. *Cvx: Matlab software for disciplined convex programming*, 2008.
- [6] W.P.M.H. Heemels, Karl Henrik Johansson, and Paulo Tabuada. An introduction to event-triggered and self-triggered control. In *IEEE 51st Annual Conference on Decision and Control (CDC)*, pages 3270–3285, 2012.
- [7] Kazufumi Ito and Karl Kunisch. Optimal control with $L^p(\Omega)$, $p \in [0, 1)$, control cost.
- [8] Fu Lin, Makan Fardad, and Mihailo R Jovanovi. Design of optimal sparse feedback gains via the alternating direction method of multipliers. *IEEE Transactions on Automatic Control*, 58(9):2426–2431, 2013.
- [9] Manuel Mazo, Adolfo Anta, and Paulo Tabuada. On self-triggered control for linear systems: Guarantees and complexity. In *European Control Conference (ECC)*, pages 3767–3772, 2009.
- [10] Nader Motee and Ali Jadbabaie. Optimal control of spatially distributed systems. *IEEE Transactions on Automatic Control*, 53(7):1616–1629, 2008.
- [11] Nader Motee and Qiyu Sun. Sparsity and spatial localization measures for spatially distributed systems. *SIAM Journal on Control and Optimization*, 55(1):200–235, 2017.
- [12] Masaaki Nagahara, Daniel E Quevedo, and Dragan Nešić. Maximum hands-off control: a paradigm of control effort minimization. *IEEE Transactions on Automatic Control*, 61(3):735–747, 2016.
- [13] Cameron Nowzari and Jorge Cortés. Self-triggered coordination of robotic networks for optimal deployment. *Automatica*, 48(6):1077–1087, 2012.
- [14] Matheus Souza, Grace Silva Deaecto, José Cláudio Geromel, and Jamal Daafouz. Self-triggered linear quadratic networked control. *Optimal Control Applications and Methods*, 35(5):524–538, 2014.